Journal of Power Sources 263 (2014) 110–117

Contents lists available at ScienceDirect

Journal of Power Sources

journal homepage: www.elsevier.com/locate/jpowsour

Calcium metaborate as a cathode additive to improve the high-temperature properties of nickel hydroxide electrodes for nickel–metal hydride batteries

Jing Li [a], Enbo Shangguan [a,*], Dan Guo [a], Quanmin Li [a], Zhaorong Chang [a,*], Xiao-Zi Yuan [b], Haijiang Wang [b]

[a] Collaborative Innovation Center of Henan Province for Green Manufacturing of Fine Chemicals, School of Chemistry and Chemical Engineering, Henan Normal University, Xinxiang 453007, PR China
[b] National Research Council of Canada, Vancouver, BC V6T 1W5, Canada

HIGHLIGHTS

- $Ca(BO_2)_2$ is proposed as a cathode additive to improve the Ni–MH cell performance.
- $Ca(BO_2)_2$ facilitates a more uniform distribution of Ca than other calcium additives.
- The cells with $Ca(BO_2)_2$ show excellent electrochemical performance at 25 and 70 °C.

ARTICLE INFO

Article history:
Received 23 January 2014
Received in revised form
14 March 2014
Accepted 26 March 2014
Available online 18 April 2014

Keywords:
Nickel–metal hydride battery
High-temperature performance
Soluble calcium salt
Calcium metaborate
Cycle stability

ABSTRACT

In this paper, a novel additive, calcium metaborate (CMB), is proposed to improve the high-temperature characteristics of the nickel electrodes for nickel–metal hydride batteries. As a soluble calcium salt, CMB can easily and uniformly be dispersed in the nickel electrodes. The effects of CMB on the nickel electrode are investigated via a combination of cyclability, capacity retention, electrochemical impedance spectroscopy, scanning electron microscope and X-ray diffraction. Compared with conventional nickel electrodes, the electrode containing 0.5 wt.% CMB exhibits superior electrode properties including enhanced discharge capacity, improved high-rate discharge ability and excellent cycle stability at an elevated temperature (70 °C). The improved cell performance of the nickel electrode containing CMB additives can be attributable to the increased oxygen evolution overvoltage and slower oxygen evolution rate. Compared with insoluble calcium salts, such as $Ca(OH)_2$, $CaCO_3$, and CaF_2, CMB is more effective as a cathode additive to improve the high-temperature performance of Ni–MH batteries.

1. Introduction

Nickel–metal hydride (Ni–MH) batteries have been intensively studied and widely used in today's power tools and portable applications due to its high rate charge/discharge capability, flexible design capability for demands, and environmentally friendly nature [1–6]. Although Ni–MH batteries are commercially available, further research is still required to improve their high-temperature performance for applications in electric vehicles (EV) and hydride electric vehicles (HEV) [7,8]. As is well known, the high-temperature and high power performance is one of the key requirements for a Ni–MH power battery, and is strongly affected by the high-temperature performance of nickel hydroxide electrodes. At elevated temperatures, the undesirable oxygen evolution reaction on the positive electrode, which results in lower charge efficiency, is the main factor that restricts the high-temperature performance of the positive electrode at a high charge/discharge rate. Consequently, the capacity of Ni–MH batteries quickly fades with increased internal resistance and decreased cycle life [7,8].

To enhance the high-temperature characteristics of Ni–MH batteries, considerable attempts have been made to improve the performance of nickel electrodes, which are classified as follows:

1) cobalt and its compounds, such as metallic Co [9,10], $Co(OH)_2$ [11,12], and CoOOH [13,14], which are the indispensable

* Corresponding authors. Tel.: +86 373 3326335; fax: +86 373 3326336.
E-mail addresses: shangguanenbo@163.com (E. Shangguan), czr_56@163.com (Z. Chang).

http://dx.doi.org/10.1016/j.jpowsour.2014.03.134
0378-7753/

components in the positive electrodes of Ni-MH batteries to achieve high electrochemical efficiency.

2) rare earth elements (Y, Er, and Lu, *etc.* [15–18]), rare earth oxides (Y, Er, and Lu oxides, *etc.* [19,20]) and rare earth hydroxides (yttrium hydroxide [21–24], ytterbium hydroxide [25], and lutetium hydroxide [26]), which have remarkable properties that can shift the oxygen evolution potential of nickel electrodes to positive values.
3) calcium compounds, such as CaF_2 [27], $CaCO_3$ [28], $Ca(OH)_2$ [29,30], and $Ca_3(PO_4)_2$ [31], which are effective additives to raise the oxygen evolution potential of nickel electrodes, suppressing the formation of γ-NiOOH that leads to the harmful expansion of β-$Ni(OH)_2$ electrodes.

Nevertheless, although the high-temperature characteristics of Ni–MH batteries can be significantly improved by the aforementioned methods, the results are still not satisfying. For EV applications, the cost is a very important factor to be considered. The use of rare earth elements doping or coating greatly increases the cost of Ni–MH batteries. Thus, the cheap calcium compounds are more promising as cathode additives for Ni–MH batteries. To date, calcium compounds used in the nickel electrodes are usually insoluble calcium salts, such as CaF_2, $CaCO_3$, $Ca(OH)_2$, and $Ca_3(PO_4)_2$. For example, Derek et al. [27] have studied the effect of CaF_2 on the high-temperature charge acceptance of $Co(OH)_2$-coated $Ni(OH)_2$ electrode for Ni–MH batteries and concluded that the use of CaF_2 additive in the positive electrode could significantly reduce gas evolution and improve the high-temperature stability. However, the small amounts (0.5–5 wt.%) of such additives with submicron sizes are not easily and uniformly mixed with a mass of nickel hydroxide powder with a particle size of 5–15 μm in an agglomeration. As is well known, the uniformity of additives in active materials greatly affects the physical and electrochemical performance of the electrode. Therefore, a simpler and more economical method of improving the dispersancy of calcium compounds in the positive electrode is desirable.

Soluble calcium salts, which can dissolve in the slurry during the mixing process and result in a homogeneous dispersal in the active materials, may be a good choice to solve the problem. When the alkaline electrolyte is added into the assembled battery with the nickel electrode containing soluble calcium salts, Ca^{2+} of the soluble calcium salts can react with OH^- in the alkaline electrolyte. The reaction equation is as follows:

$$Ca^{2+} + 2OH^- = Ca(OH)_2\downarrow \quad (1)$$

Therefore, soluble calcium salts act similar to $Ca(OH)_2$, which raises the oxygen evolution potential of the nickel electrode, and minimizes the shape change of the nickel electrode. Especially, one of the advantages of using soluble calcium salts is that additives can be easily mixed with active materials and the distribution of Ca^{2+} can be greatly improved.

Up to now, few studies have been reported on the application of soluble calcium salts as cathode additives in nickel electrodes for Ni–MH batteries. This is because that the use of common soluble calcium salts, such as $CaCl_2$, and $Ca(NO_3)_2$, introduces harmful anions, which are detrimental to the properties of Ni–MH batteries. For instance, it was found that NO_3^- could bring about so called "shuttle reactions" and result in a capacity drop of the battery during storage [32]. So, selection of suitable soluble calcium salts and investigation of their effects on the high-temperature performance of Ni-MH batteries are of great interest.

In our previous work, we have reported a novel economical approach to increase the high-temperature charge acceptance of the positive electrode through the use of sodium metaborate ($NaBO_2$) as an electrolyte additive [33]. It was found that BO_2^- could effectively improve the high-temperature performance of Ni–MH batteries. In this work, on the basis of the above research calcium metaborate (CMB), a soluble calcium salt, was selected as cathode additives in an attempt to improve the high-temperature electrochemical performance of Ni–MH batteries. The effects of CMB on the electrochemical performance of the Ni–MH battery were investigated. For comparison, other calcium additives of submicron $Ca(OH)_2$, $CaCO_3$, and CaF_2 were also included in the test.

2. Experimental

2.1. Preparation of nickel electrodes and cell assembly

The pasted nickel electrodes (E_A) were prepared as follows: 84.5 wt.% spherical β-$Ni(OH)_2$, 5.0 wt.% CoO, 5.0 wt.% nickel powder, and 0.5 wt.% CMB were thoroughly mixed with a certain amount of 5.0 wt.% hydroxypropyl methylcellulose (HPMC) and polytetrafluoroethylene (PTFE) solution as a binder to obtain a homogeneous slurry possessing adequate rheological properties. The mixed slurry was poured into a foam nickel sheet (2 cm × 2 cm) and dried at 80 °C for 5 h. Subsequently, the pasted electrodes were pressed at a pressure of 20 MPa for 3 min. For comparison, the conventional electrode without CMB additives (E_B) and electrodes with other calcium additives (0.5 wt.% of submicron $Ca(OH)_2$(E_C), $CaCO_3$(E_D), and CaF_2(E_E))were prepared using the same method. The spherical β-$Ni(OH)_2$ used in this work is a commercial product (Henan Kelong Co., Ltd., China).

2.2. Electrochemical measurements

Galvanostatic charge–discharge tests were conducted using a Land CT2001A battery performance testing instrument (Wuhan Jinnuo Electronics Co. Ltd, China). For activation, five charge/discharge cycles at 0.2 C were performed, and the cells were discharged to 1.0 V. The batteries were then charged at a 1 C rate for 72 min and separately discharged at respective 0.2, 1, 2 C and 5 C discharge current rates under room and an elevated temperature (25 °C and 70 °C). The cut-off voltages were set as 1.0 V, 1.0 V, 0.9 V, 0.7 V, respectively. In the subsequent charge–discharge cycling tests, the batteries were charged at a 1 C rate for 72 min, rested for 10 min, and then discharged at respective 1 and 5 C discharge current rates. The cut-off voltages were set as 1.0 and 0.7 V, respectively.

Cyclic voltammogram (CV), electrochemical impedance spectroscopy (EIS), and steady-state polarization measurements were conducted in a three-electrode model cell at 25 °C and 70 °C, respectively, using a Solartron SI 1260 impedance analyzer with a 1287 potentiostat interface. The test cell comprised a working electrode (the positive electrode), a counter electrode (nickel ribbon), an Hg/HgO reference electrode, and 6 M KOH + 15 g L^{-1} LiOH solution as electrolyte. For CV test, the scanning rate was between 1 mV s^{-1} and 8 mV s^{-1} over a potential range from 0.0 V to 0.8 V. For EIS measurement, the impedance spectra were recorded at an AC signal of 5 mV in amplitude as the perturbation with a sweep frequency range of 100 kHz–10 mHz. Steady-state polarization measurements were performed as follows: after the nickel electrode was fully charged at a rate of 0.2 C, it was polarized at constant potentials in 25 mV steps from 0.45 to 0.65 V vs. Hg/HgO. At each potential, the electrodes were polarized for 10 min and steady state currents were recorded.

2.3. Characterization techniques for the nickel electrodes

The morphology of the nickel electrodes were determined by scanning electron microscopy (SEM) (JEOL-JSM-6701F). The phase

distribution and composition was determined via energy dispersive X-ray (EDX) spectrometer attached to the SEM. X-ray diffraction (XRD) was performed on a D8 diffractometer (Bruker, Germany) employing Cu Kα radiation. The scan data were collected in a 2θ range of 5–70°. The step size was 0.026° with a counting time of 3 s.

In all the above experiments, the reagents used were of A.R. grade and the electrolyte was prepared with deionized water.

3. Results and discussion

3.1. Effects of CMB additives on the distribution of calcium

To investigate the effects of different calcium additives on the positional distribution of calcium in the nickel electrodes, surface analysis of the electrodes with CMB or $Ca(OH)_2$ after 10 cycles at a 1 C rate at 70 °C was performed by SEM and EDX mapping, as shown in Fig. 1. From the SEM images (Fig. 1(a) and (c)), it can be found that electrodes (a) and (b) with different additives have a similar morphology. However, element mapping obtained by the EDX analysis (Fig. 1(b) and (d)) shows that the distribution of Ca on the surface of nickel electrodes significantly differs. Obviously, calcium elements on the surface of the electrode with CMB additives are homogeneously distributed on the cathode. In contrast, on the surface of the electrode with $Ca(OH)_2$ additives, calcium elements are unevenly distributed. The result suggests that soluble calcium salt CMB is more promising as cathode additives in terms of the dispersal. Thus, the proposed method is capable of fabricating a cathode with well-dispersed calcium additives.

3.2. Effects of CMB additives on the charge/discharge performance

To ascertain the effects of various additive contents of CMB on the electrochemical performance of nickel electrodes, the relationship between the discharge capacity and the amount of CMB added at rates of 0.2 C, 1.0 C, 2.0 C and 5.0 C at 25 and 70 °C is shown in Fig. 2. Obviously, at 70 °C for all the discharge rates (0.2, 1.0, 2.0 and 5.0 C) the nickel hydroxide electrodes with CMB additives exhibit higher discharge capacity than those without additives. This

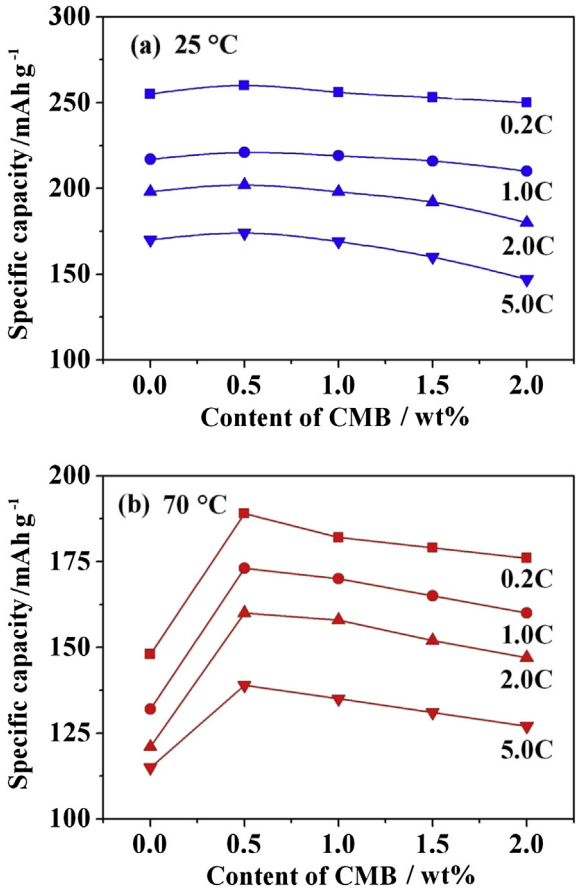

Fig. 2. Variation of the discharge capacity against the amount of CMB added to the nickel electrodes under different discharge rates at (a) 25 °C and (b)70 °C.

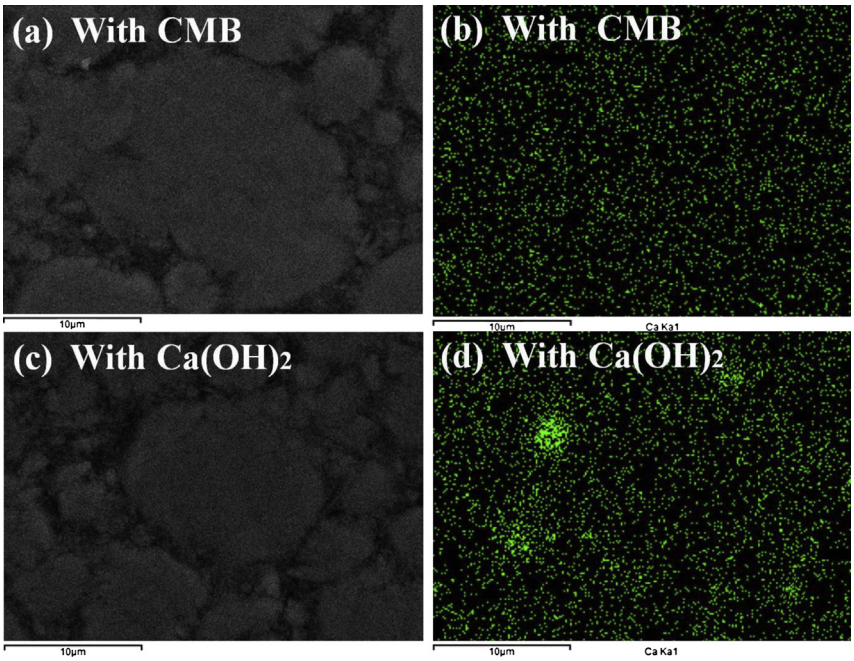

Fig. 1. SEM back scattering electron images and EDS elemental mappings of the nickel electrodes with 0.5 wt.% CMB(a, b) and $Ca(OH)_2$ (c, d) additives.

indicates that the introduction of CMB seems to be a key factor for improving the discharge capacity at an elevated temperature. As seen in Fig. 2, the discharge capacity at an elevated temperature significantly increases with the addition of CMB and peaks at a $Ca(OH)_2$ concentration of 0.5 wt.%, while further increase in the CMB amount beyond 0.5 wt.% results in a decrease in discharge capacity. At 25 °C the discharge capacity also slightly increases with increasing the contents of CMB in nickel electrodes until the addition amount of CMB reaches up to 0.5 wt.%, while further increase in the CMB amount results in a slight decrease in the discharge capacity. Previously, we have assumed that CMB added into the electrode acts similar to $Ca(OH)_2$, which is electrochemically inactive. An excessive amount of CMB can lead to a decrease in the discharge capacity because of its poor conductivity and lack of electrochemical capacity. Consequently, the optimum additive amount of CMB is found to be around 0.5 wt.% at both 25 and 70 °C.

Fig. 3 compares the discharge curves of nickel electrodes with 0.5 wt.% CMB and without CMB at different discharge rates at 25 °C and 70 °C.

As can be clearly seen in Fig. 3(b), at an elevated temperature (70 °C), electrode A with CMB additives exhibits a higher discharge capacity and higher discharge potential plateau than the regular electrode B without CMB additives at the same discharge rates (0.2 C, 1.0 C, 2.0 C and 5.0 C). For example, at a rate of 0.2 C, the discharge capacity of electrode A is 188.8 mAh g^{-1} in comparison with 146.0 mAh g^{-1} for electrode B. At 5.0 C, electrode A shows a higher discharge capacity of 139.5 mAh g^{-1}, whereas the value for electrode B is only 114.4 mAh g^{-1}. The utilization of $Ni(OH)_2$ at a high temperature is greatly improved by adding CMB compounds. Furthermore, from Fig. 3(a), it can be found that cell A shows a slightly higher discharge capacity than the regular cell B at 25 °C,

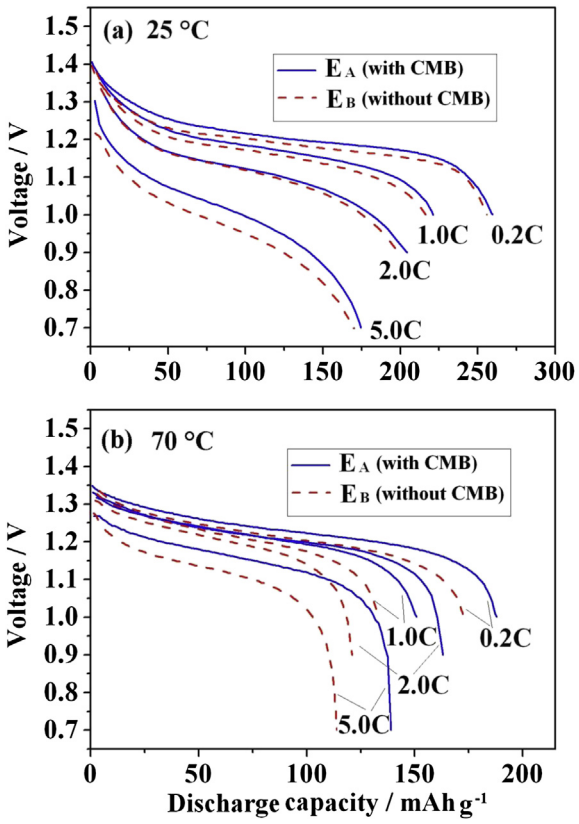

Fig. 3. Discharge curves of Ni-MH cells using the nickel electrodes (E_A) and (E_B) with/without 0.5 wt.% CMB additives at different discharge rates at (a) 25 °C and (b) 70 °C.

indicating that the studied additive at an optimum amount has a positive effect on the discharge performance of Ni–MH batteries at room temperature.

3.3. Effects of CMB additives on the cycling performance

The electrochemical performance of nickel electrodes with and without 0.5 wt.% CMB addition was further investigated by cyclability measurements. For comparison, the nickel electrodes with 0.5 wt.% submicron $Ca(OH)_2$, $CaCO_3$ and CaF_2 were also included in the test. Fig. 4 compares the cycle stability of different nickel electrodes at a 1 C rate at 25 and 70 °C.

At both 25 and 70 °C, electrode A with 0.5 wt.% CMB exhibits the highest specific capacity and better cycling stability than the regular electrode B during the cycling processes. From Fig. 4(a), it can be seen that the maximum discharge capacity for electrode A is 223.7 mAh g^{-1} and then gradually decreases to 220.4 mAh g^{-1} (98.5% of its maximum) at the 200th cycle, while the maximum discharge capacity for electrode B is only 217.8 mAh g^{-1} with only 212.2 mAh g^{-1} (97.4% of its maximum) remained at the 200th cycle. To quantitatively characterize the cyclic stability of the cells, the deterioration rate (R_d) is used, where R_d is equal to $(C_m - C_i)/C_m$ (C_m: maximum capacity; C_i: capacity at a certain cycle). As seen in Fig. 4, the R_d at the 200th cycle (1 C) for electrodes A, B, C, D and E are 98.5%, 97.4%, 96.5%, 94.2% and 92.6%, respectively, which indicates that electrode A with a CMB addition has a much better cyclic stability and higher discharge capacity than the electrodes with other calcium additives. The result also suggests that CMB has a positive effect on the cycling performance of Ni–MH batteries at room temperature.

In Fig. 4(b), it is clear that at 70 °C the discharge capacity for electrode A is significantly higher than for the other electrodes in all cycles. It can also be seen that the maximum discharge capacity for electrode A is 177.6 mAh g^{-1} and then gradually decreases to 155.8 mAh g^{-1} (87.7% of its maximum) at the 50th cycle, while the maximum discharge capacity for electrode B is only 132.2 mAh g^{-1} with only 91.9 mAh g^{-1} (69.5% of its maximum) remained at the 50th cycle. In contrast, electrodes C (with $Ca(OH)_2$), D (with $CaCO_3$), and E (with CaF_2) also exhibit improved cycling performance with retained discharge capacities of 130.2, 114.1 and 102.8 mAh g^{-1} (76.5, 68.7 and 59.3% of the initial capacities), respectively, after 50 cycles. Compared with electrodes C–E, electrode A containing CMB exhibits the highest specific capacity and better cycling stability, indicating that CMB is more effective to improve the performances of Ni–MH batteries. The improvement may be ascribed to the uniform distribution of Ca in the pasted nickel electrode and the useful anion of BO_2^- [33].

3.4. SEM images and XRD patterns of electrodes after charge/discharge cycles

To further investigate the effect of the CMB on the nickel electrodes during the charge/discharge cycles, surface analysis of electrodes A (with CMB) and B (without CMB) after certain cycles at 1 C rate at 25 and 70 °C was performed by SEM, as shown in Fig. 5. From the SEM images, it can be seen that after 200 cycles at 25 °C electrodes A and B have a comparatively compact surface morphology. However, after 50 cycles at 70 °C, for both electrodes, some active materials were severely separated from the electrode surface. This implies that the abrupt degradation of the discharge capacity of electrodes A and B at a high temperature, as shown in Fig. 5, appears to be associated with the loss of active materials. Additionally, the electrodes after 50th cycles at 70 °C are looser than those after 200th cycles at 25 °C, indicating that the structure and surface morphology of the electrode undergo more changes

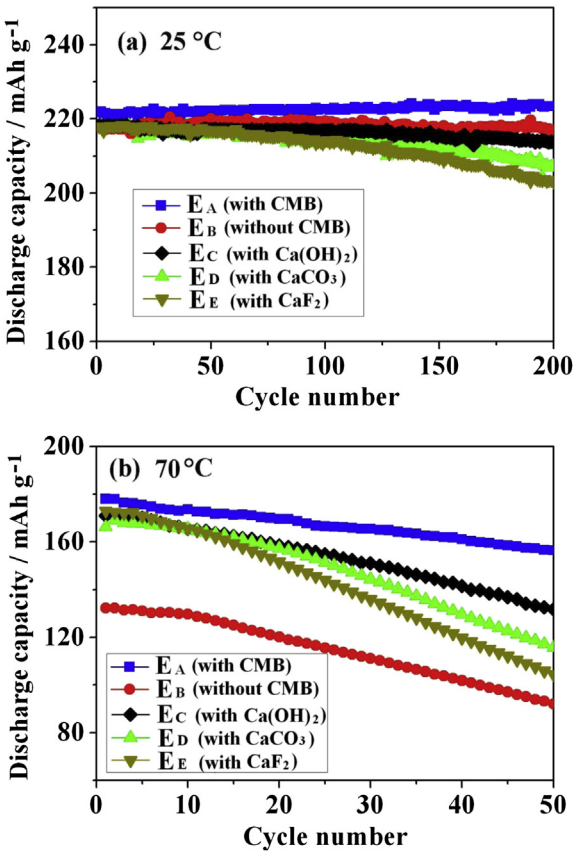

Fig. 4. Cyclic performance of Ni–MH cells using different nickel electrodes at 1 C charge/discharge current rate at (a) 25 °C and (b)70 °C.

with the increase in temperature. Comparing electrode A (Fig. 5a and c) and electrode B (Fig. 5c and d), it can be found that the surface morphology of electrode B appears to be more porous with better defined holes or pores. This indicates that the CMB additive

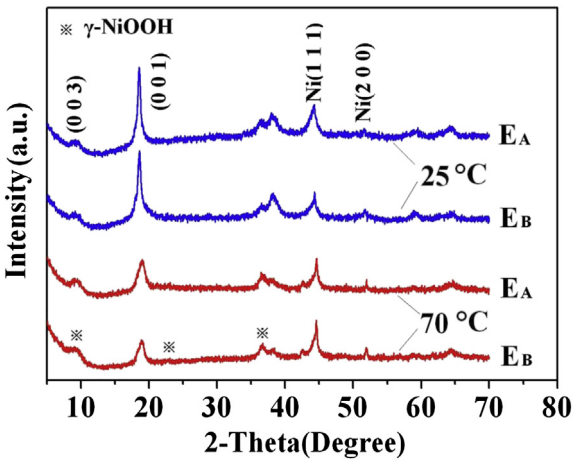

Fig. 6. XRD patterns of the nickel electrodes (E_A) with and (E_B) without 0.5 wt.% CMB additive after cycles at 1 C. (a) after 200th cycles at 25 °C; (b) after 50th cycles at 70 °C.

has a positive effect on the surface morphology of electrodes, which may result from the suppression of the γ-NiOOH formation and the less impacts from oxygen gas.

In order to study the structural transformation during the charge/discharge process at both 25 and 70 °C, the XRD patterns of nickel electrodes A and B after cycles at a 1 C rate are compared in Fig. 6. Obviously, diffraction peaks from the γ-phase nickel oxyhydroxide can be detected for both nickel electrodes after cycles at both 25 and 70 °C. It is well known that the positive electrode in the Ni-MH battery can be degraded by the swelling of the electrode resulting from the transformation of β-NiOOH to γ-NiOOH [34,35]. The (0 0 1) and the (0 0 3) peaks from β-NiOOH and γ-NiOOH, respectively, have the highest intensities, which appear even when small amounts of these phases are present. For comparison, a ratio between the two peaks is taken to obtain sensitivity of these two species to XRD [35]. On the patterns of electrode A after cycles at 25 and 70 °C, the relative intensity of γ-NiOOH (0 0 3) and β-NiOOH (0

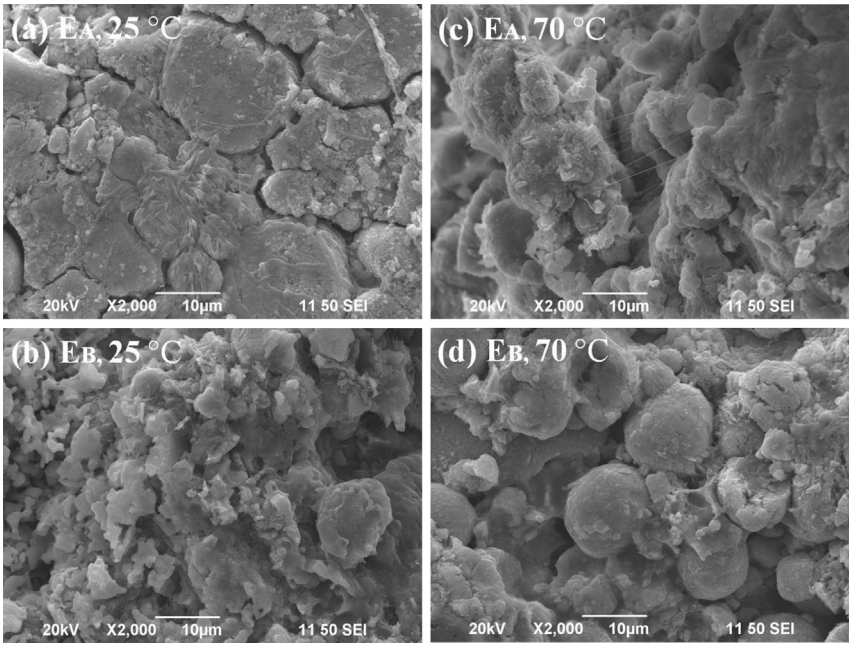

Fig. 5. SEM micrographs of the nickel electrodes (E_A) and (E_B) with/without 0.5 wt.% CMB additives at 1 C. (a) E_A, after 200 cycles at 25 °C; (b) E_B, after 200 cycles at 25 °C; (c) E_A, after 50 cycles at 70 °C; (d) E_B, after 50 cycles at 70 °C.

0 1) is 45:100 and 70:100, respectively; however, on the patterns of electrode B, the value is 52:100 and 78:100, respectively. Furthermore, it is worth noting that although the cycle's time at 70 °C is shorter than that at 25 °C, the formed amount of γ-NiOOH after cycles at 70 °C is more than that at 25 °C. This implies that the capacity fading during the charge/discharge process at a high temperature, most likely, results from the formation of γ-NiOOH. To some extent the use of CMB additives can suppress the formation of γ-NiOOH and reduce the swelling of nickel electrodes during the charging/discharging processes at room temperature and an elevated temperature.

All the results suggest that the addition of CMB plays an important role in improving the high-temperature performance of nickel hydroxide electrodes. To understand how the CMB additive affects the electrochemical performance of nickel electrodes, the electrochemical performance of nickel electrodes with and without 0.5 wt.% CMB additives was further studied by CV, EIS and steady-state polarization measurements.

3.5. Effects of CMB additives on cyclic voltammogram

Fig. 7 illustrates the stable CV curves of electrodes A (with CMB) and B (without CMB) at various scan rates at 25 °C and 70 °C, respectively. Obviously, for both nickel electrodes, one anodic nickel hydroxide oxidation peak and one cathodic oxyhydroxide reduction peak are observable on the CV curves. To compare the CV characteristics of both electrodes, the results of CV measurements at a scan rate of 1 mV s^{-1} are tabulated in Table 1. Generally, the potential difference ($\Delta(E_{O-R})$) between the oxidation (E_O) and reduction (E_R) potentials is a measure of the reversibility of the redox reaction [33]. Smaller $\Delta(E_{O-R})$ suggests that the electrode reaction is more reversible. At 70 °C, the $\Delta(E_{O-R})$ value for electrode A is 137 mV, while that for the reference electrode B is 160 mV. At 25 °C, the $\Delta(E_{O-R})$ value of electrode A is 166 mV, which is a little smaller than that of electrode B. The result implies that CMB can efficiently improve the reaction reversibility at room temperature and at an elevated temperature, which is in agreement with the previous cycling test (see Fig. 4).

Table 1
Electrochemical parameters obtained from the CV curves of the nickel electrodes A and B.

Temperature	Electrode	Additive	E_O (mV)	E_R (mV)	E_{oe} (mV)	$\Delta(E_{O-R})$ (mV)	$\Delta(E_{oe-O})$ (mV)
25 °C	E_A	CMB	468	302	596	166	128
	E_B	No	477	306	581	171	104
70 °C	E_A	CMB	455	318	568	137	113
	E_B	No	460	300	537	160	77

$\Delta(E_{oe-O})$, an important parameter for estimating the electrochemical properties of the electrodes [17,18], is defined as the potential difference between the oxygen evolution potential (E_{oe}) and oxidation potential (E_O), and is usually used as an indicator of charge efficiency and charge acceptance. The large $\Delta(E_{oe-O})$ value facilitates the electrode to be charged fully before oxygen evolution. Thus, the greater the $\Delta(E_{oe-O})$, the better the charge efficiency and charge acceptance. As shown in Table 1, at 70 °C, the $\Delta(E_{oe-O})$ value for electrode A is 113 mV, while that for the reference electrode B is 77 mV. Moreover, it is noteworthy that at 25 °C, the $\Delta(E_{oe-O})$ of the electrode with 0.5 wt.% CMB is higher than that of the electrode without additives, indicating that the use of CMB additives is also beneficial to the decrease in oxygen evolution and the improvement of the charge acceptance at room temperature. This is in good agreement with the results from the charge/discharge test.

As is known, the electrochemical reaction process of a nickel hydroxide electrode is limited by the proton diffusion through the lattice [36]. Therefore, it is of great importance to study the nickel electrode's proton diffusion coefficient. The proton diffusion coefficient of the $Ni(OH)_2$ electrode was estimated based on the CV tests. In the case of semi-infinite diffusion, the peak current, i_p, may be expressed by the classical Randles–Sevcik equation [36]:

$$i_p = 2.69 \times 10^5 \times n^{3/2} \times A \times D^{1/2} \times C_0 \times v^{1/2} \quad (2)$$

where n is the electron number of the reaction (≈ 1 for β-$Ni(OH)_2$), A is the surface area of the electrode, D is the diffusion coefficient, v

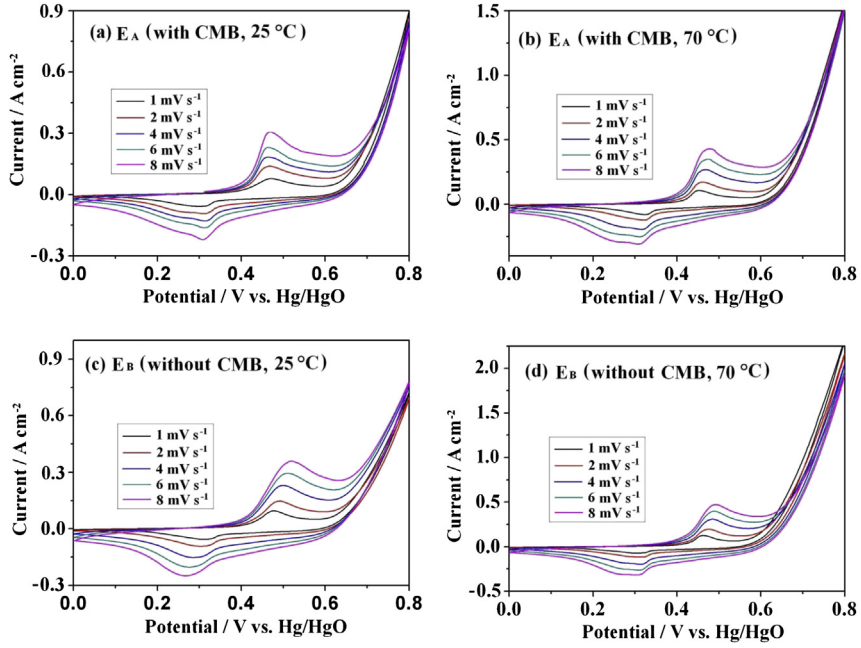

Fig. 7. CV curves of the nickel electrodes (E_A) and (E_B) with/without 0.5 wt.% CMB additives at different scan rates at 25 °C and 70 °C.

is the scanning rate, and C_0 is the initial concentration of the reactant. For a $Ni(OH)_2$ electrode,

$$C_0 = \rho/M \quad (3)$$

where ρ and M are, respectively, the density and the molar mass (92.7 g mol^{-1}) of $Ni(OH)_2$.

Fig. 8 shows the relationship between the cathodic peak current (i_p) and the square root of the scan rate ($v^{1/2}$) for both nickel electrodes. As seen, good linear relationships between i_p and $v^{1/2}$ can be observed for all the electrodes, which confirms that the electrode reaction of nickel hydroxide is controlled by proton diffusion.

The proton diffusion coefficients in the two electrodes are calculated using the slopes of the fitting line in Fig. 8 based on Eq. (2). At 25 °C, it is found that the proton diffusion coefficients for electrode A are 8.984×10^{-9} cm^2 s^{-1} (25 °C) and 1.4334×10^{-8} cm^2 s^{-1} (70 °C), which are slightly larger than for electrode B (6.995×10^{-9} cm^2 s^{-1} (25 °C) and 1.1938×10^{-8} cm^2 s^{-1} (70 °C)), respectively. Clearly, to some extent proton diffuses faster in electrode A than in electrode B, which indicates that the electrode with CMB additives has higher electrochemical activity and faster reaction kinetics. Therefore, the CMB additives should take the credit for the better electrochemical properties at room temperature and at a high temperature (70 °C).

3.6. Effects of CMB additives on electrochemical impedance spectra

After the electrodes were charged and discharged for 5 cycles at a rate of 1 C, the electrochemical impedance spectra were measured at the open circuit potential at 25 °C and 70 °C. Fig. 9 presents the EIS plots of electrodes A (with CMB) and B (without CMB). It can be seen that the Nyquist plots of both electrodes display a depressed semicircle resulting from charge-transfer resistance in the high frequency region, and a slope related to Warburg impedance in the low-frequency region [33,37]. To obtain the charge-transfer resistance of the electrodes, an equivalent circuit is used to fit these experimental data as shown in Fig. 9(a), in which R_s represents the total resistance of the solution, CPE is the constant phase element related to the double layer capacitance, R_{ct} is the charge-transfer resistance of the electrode, and W is the generalized finite Warburg impedance (Z_w) of the solid phase diffusion. Table 2 shows the best fitting results of the elements based on the equivalent circuit. As previously discussed, CMB added into the electrode acts similar to $Ca(OH)_2$. However, $Ca(OH)_2$ are electrochemically inactive and possibly, jamming the passages for ion transfers and reducing the contact surface for the electrochemical reaction [30]. So, it is of more interest to study the effect of CMB on the electron transfer resistance, R_{ct}, which relates to the electrochemical reactions. It can be clearly seen from Table 2 that the R_{ct} values of electrode A with CMB are slightly higher than those of electrode B without CMB at both 25 °C and 70 °C, respectively. This implies that CMB has a negligible negative effect on the electron transfer resistance of nickel electrode. In other words, the electrochemical reaction on the electrodes with CMB proceeds as fast as that on those without CMB. This is in agreement with the results of the CV measurements and charge/discharge testing. The CPE is related to double electric layer and may be affected by surface roughness of solid electrodes [38]. It can be seen that the CPE of electrode A are relatively higher than those of electrode B. This may be resulted from the use of CMB, the electrodes exhibit efficiently active surface area for the electrochemical reactions.

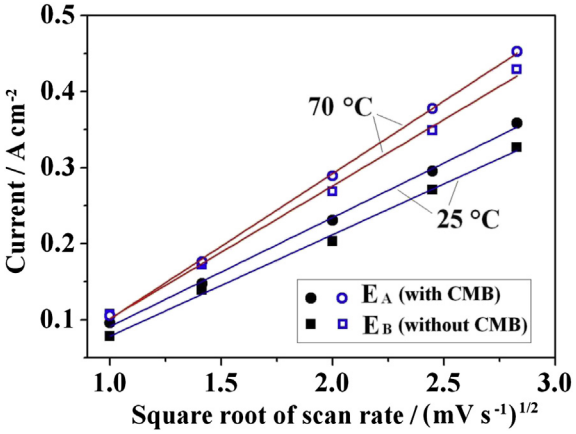

Fig. 8. Linear relationship between the cathodic peak current and the square root of scan rate for the nickel electrodes (E_A) and (E_B) with/without 0.5 wt.% CMB additives.

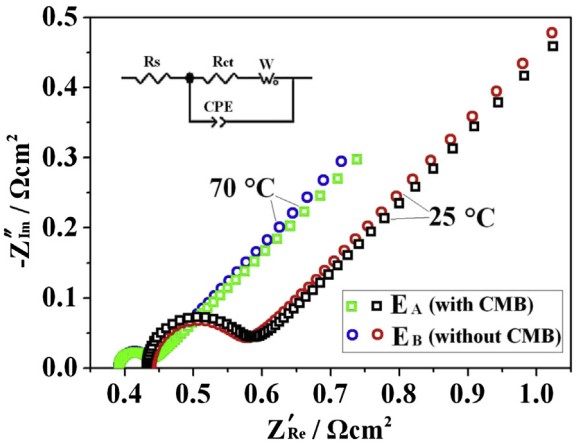

Fig. 9. Electrochemical impedance spectra of the nickel electrodes (E_A) and (E_B) with/without 0.5 wt.% CMB additives measured at the open circuit potential at 25 °C and 70 °C.

3.7. Effects of CMB additives on the polarization

To assess effects of CMB on the oxygen evolution reaction (OER) on the nickel electrode, steady-state polarization measurements were performed at 25 °C. Fig. 10 shows the variation of the steady state polarization current to the potential. It is clear that the electrode A with CMB additives shows lower currents than that without additives at both temperatures, indicating the oxygen evolution rate on electrode A is slower. From Fig. 10 one can see that at 0.65 V versus Hg/HgO electrode, the current of oxygen evolution on electrodes A and B are 59.8 mA and 40.0 mA, respectively, clearly indicating that the controlling/inhibition of OER on electrode A is much stronger than that on electrode B. Thus, electrode A suffers less impact from the produced oxygen gas. Moreover, it is found that the surface of electrode B is much coarser than that of electrode A as observed with naked eyes, showing the former suffers more impacts from oxygen gas. Thus, it can be concluded that the use of CMB can effectively suppress the oxygen evolution and then the nickel electrode suffers less impact from oxygen gas.

On the basis of these facts, it has been proved that CMB can be used as an effective cathode additive to improve the high-temperature performance of Ni–MH batteries, including the discharge capacity, high-rate discharge ability, and cycle stability. On the one hand, CMB is capable of not only increasing oxygen evolution overpotential but also decreasing the oxygen evolution rate. Oxygen evolution can be remarkably inhibited by the addition of CMB to the electrode. To some extent the solid-state diffusion

Table 2
Parameters obtained from the EIS plots of the nickel electrodes A and B.

Electrode	Additive	25 °C				70 °C			
		R_s (Ω cm^2)	CPE (F cm^{-2})	R_{ct} (Ω cm^2)	W (Ω cm^2)	R_s (Ω cm^2)	CPE (F cm^{-2})	R_{ct} (Ω cm^2)	W (Ω cm^2)
E_A	CMB	0.4307	0.05424	0.1712	6.768	0.3804	0.04359	0.08717	6.211
E_B	no	0.4354	0.05612	0.1703	6.121	0.3832	0.04625	0.08692	4.665

processes are improved, leading to a higher electrochemical activity, as indicated by CV and steady-state polarization measurements. On the other hand, CMB shows less negative effect on the charge resistance of the nickel electrode, which may be attributed to the better dispersal of calcium in the electrodes and the introduction of useful anion BO^{2-}. These benefits lead to higher charge efficiency and excellent discharge ability of the nickel electrode at room temperature and an elevated temperature. It is also found that CMB is greatly beneficial to the enhancement of the high-temperature performance of Ni–MH cells than the other calcium additives. As expected, a uniform distribution of CMB in the pasted nickel electrode significantly increases the high-temperature charge acceptance of the nickel electrodes at high temperatures without other negative effects, such as the increase in the charge transfer resistance.

4. Conclusions

The high-temperature charge/discharge performance of Ni–MH batteries was successfully improved by the introduction of CMB. Compared with conventional cells, the in-house prepared cells exhibit an enhanced discharge capacity, improved high-rate discharge ability and excellent cycle stability at room temperature and an elevated temperature (70 °C). EDX studies show that a pasted nickel electrode with a uniform distribution of Ca can be easily prepared by the proposed method. EIS studies show that CMB has little negative effect on the electron transfer resistance of nickel electrode. CV and steady-state polarization tests indicate that CMB can efficiently enhance the oxygen evolution overvoltage and depress the oxygen evolution, leading to a higher charge acceptance and proton diffuse coefficient. Compared with insoluble calcium salts ($Ca(OH)_2$, $CaCO_3$, and CaF_2), CMB is more effective to improve the performances of Ni–MH batteries. It is believed that this distinctive approach is promising and effective for high-temperature and high-rate electrochemical performance improvement of rechargeable alkaline Ni–MH batteries.

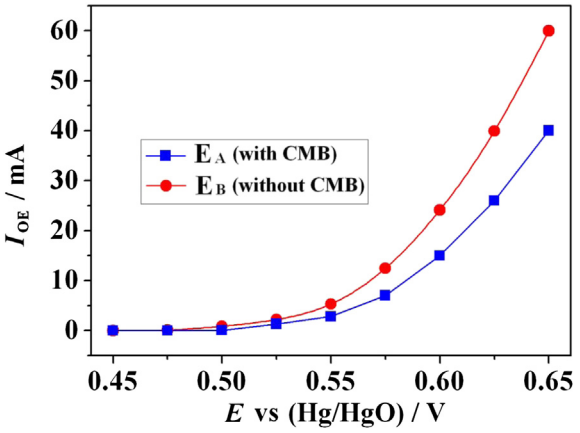

Fig. 10. Variations of the steady state polarization current to the potential for the nickel electrodes (E_A) and (E_B) with/without 0.5 wt.% CMB additives.

Acknowledgments

The authors thank the financial supports from the Joint Funds of the National Natural Science Foundation of China (No. U1304211), Henan Education Bureau Foundation of China (Nos. 13A150507 and 13A150512), Henan Provincial Department of Science and Technology Foundation of China (Nos. 132300410294 and 132300410299) and Henan Key Science and Technology Program of China (No. 132102210256).

References

[1] K. Watanabe, M. Koseki, N. Kumagai, J. Power Sources 58 (1996) 23–28.
[2] U. Kohler, C. Antonius, P.B. Uerlein, J. Power Sources 127 (2004) 45–52.
[3] T.N. Ramesh, P. Vishnu Kamath, J. Power Sources 156 (2006) 655–661.
[4] M.A. Fetcenko, S.R. Ovshinsky, B. Reichman, K. Young, C. Fierro, J. Koch, A. Zallen, W. Mays, T. Ouchi, J. Power Sources 165 (2007) 544–551.
[5] M.A. Kiani, M.F. Mousavi, S. Ghasemi, J. Power Sources 195 (2010) 5794–5800.
[6] E.B. Shangguan, Z.R. Chang, H.W. Tang, X.Z. Yuan, H.J. Wang, J. Power Sources 196 (2011) 7791–7796.
[7] C. Fierro, A. Zallen, J. Koch, M.A. Fetcenko, J. Electrochem. Soc. 153 (2006) A492–A496.
[8] E.B. Shangguan, J. Li, Z.R. Chang, H.W. Tang, X.Z. Yuan, H.J. Wang, Int. J. Hydrogen Energy 38 (2013) 5133–5138.
[9] X.Y. Wang, H. Luo, H.P. Yang, P.J. Sebastian, S.A. Gamboa, Int. J. Hydrogen Energy 29 (2004) 967–972.
[10] X.Y. Wang, J. Yan, H.T. Yuan, Z. Zhou, D.Y. Song, Y.S. Zhang, L.G. Zhu, J. Power Sources 72 (1998) 221–225.
[11] Z.R. Chang, H.W. Tang, J.G. Chen, Electrochem. Commun. 1 (1999) 513–516.
[12] S.A. Cheng, W.H. Leng, J.Q. Zhang, C.A. Cao, J. Power Sources 101 (2001) 248–252.
[13] W.K. Hu, X.P. Gao, M.M. Geng, Z.X. Gong, D. Nore′us, J. Phys. Chem. B 109 (2005) 5392–5394.
[14] Q.D. Wu, X.P. Gao, G.R. Li, G.L. Pan, T.Y. Yan, H.Y. Zhu, J. Phys. Chem. C 111 (2007) 17082–17087.
[15] Y. Morioka, S. Narukawa, T. Itou, J. Power Sources 100 (2001) 107–116.
[16] X.C. Ye, Y.J. Zhu, S.G. Wu, Z.J. Zhang, Z.J. Zhou, H.Z. Zheng, X.R. Lin, J. Rare Earths 29 (2011) 787–792.
[17] J.X. Ren, Z. Zhou, X.P. Gao, J. Yan, Electrochim. Acta 52 (2006) 1120–1126.
[18] X. Mi, X.P. Gao, C.Y. Jiang, M.M. Geng, J. Yan, C.R. Wan, Electrochim. Acta 49 (2004) 3361–3366.
[19] M. Oshitani, M. Watada, K. Shodai, M. Kodama, J. Electrochem. Soc. 148 (2001) A67–A73.
[20] Katsuhiko Shinyama, Hiroshi Nakamura, Toshiyuki Nohma, Ikuo Yonezu, J. Alloys Compd. 408 (2006) 288–293.
[21] Q.D. Wu, S. Liu, L. Li, T.Y. Yan, X.P. Gao, J. Power Sources 186 (2009) 521–527.
[22] J. Fan, Y.F. Yang, P. Yu, W.H. Chen, H.X. Shao, J. Power Sources 171 (2007) 981–989.
[23] F.Y. Cheng, J. Chen, P.W. Shen, J. Power Sources 150 (2005) 255–260.
[24] X.M. He, L. Wang, W. Li, C.Y. Jiang, C.R. Wan, J. Power Sources 158 (2006) 1480–1483.
[25] X.M. He, C.Y. Jiang, W. Li, C.R. Wan, J. Electrochem. Soc. 153 (2006) 566–569.
[26] J.X. Ren, J. Yan, Z. Zhou, X.J. Wang, X.P. Gao, Int. J. Hydrogen Energy 31 (2006) 71–76.
[27] X.Z. Zhang, Z.X. Gong, S.M. Zhao, M.M. Geng, Y. Wang, Derek O. Northwood, J. Power Sources 175 (2008) 630–634.
[28] S. Nathira Begum, V.S. Muralidharan, C. Ahmed Basha, Int. J. Hydrogen Energy 34 (2009) 1548–1555.
[29] W.Y. Li, S.Y. Zhang, J. Chen, J. Phys. Chem. B 109 (2005) 14025–14032.
[30] M. Hu, L.X. Lei, J.X. Chen, Y.M. Sun, Electrochim. Acta 56 (2011) 2862–2869.
[31] X.M. He, J.G. Ren, W. Li, C.Y. Jiang, C.R. Wan, Electrochim. Acta 51 (2006) 4533–4536.
[32] P. Leblanc, P. Blanchard, S. Senyarichb, J. Electrochem. Soc. 145 (1998) 844–847.
[33] E.B. Shangguan, J.L. Wang, J. Li, D. Guo, Z.R. Chang, H.W. Tang, X.Z. Yuan, H.J. Wang, Int. J. Hydrogen Energy 38 (2013) 10616–10624.
[34] C.Q. Wang, Z.L. Xing, N. Wang, G.X. Li, B.R. Wu, Chin. J. Power Sources 23 (1999) 328–331.
[35] D. Singh, J. Electrochem. Soc. 145 (1998) 116–120.
[36] A.H. Zimmerman, P.K. Effa, J. Electrochem. Soc. 131 (1984) 709–713.
[37] V. Mancier, A. Métrot, P. Willmann, Electrochim. Acta 41 (1996) 1259–1265.
[38] U. Rammelt, G. Reinhard, Electrochim. Acta 35 (1990) 1045–1049.